



## Warm Season Variations in the Low-Level Circulation and Precipitation over the Central United States in Observations, AMIP Simulations, and Idealized SST Experiments

SCOTT J. WEAVER\*

*Goddard Earth Sciences and Technology Center, University of Maryland, Baltimore County, Baltimore, Maryland*

SIEGFRIED SCHUBERT

*NASA Goddard Space Flight Center, Greenbelt, Maryland*

HAILAN WANG

*Goddard Earth Sciences and Technology Center, University of Maryland, Baltimore County, Baltimore, Maryland*

(Manuscript received 15 December 2008, in final form 14 May 2009)

### ABSTRACT

Sea surface temperature (SST) linkages to central U.S. low-level circulation and precipitation variability are investigated from the perspective of the Great Plains low-level jet (GPLLJ) and recurring modes of SST variability. The observed and simulated links are first examined via GPLLJ index regressions to precipitation, SST, and large-scale circulation fields in the NCEP–NCAR and North American Regional Reanalysis (NARR) reanalyses, and NASA's Seasonal-to-Interannual Prediction Project (NSIPP1) and Community Climate Model, version 3 (CCM3) ensemble mean Atmospheric Model Intercomparison Project (AMIP) simulations for the 1949–2002 (1979–2002 for NARR) period. Characteristics of the low-level circulation and its related precipitation are further examined in the U.S. Climate Variability and Predictability (CLIVAR) Drought Working Group idealized climate model simulations (NSIPP1 and CCM3) forced with varying polarities of recurring modes of SST variability.

It is found that the observed and simulated correlations of the GPLLJ index to Atlantic and Pacific SST, large-scale atmospheric circulation, and Great Plains precipitation variability for 1949–2002 are robust during the July–September (JAS) season and show connections to a distinct global-scale SST variability pattern, one similar to that used in forcing the NSIPP1 and CCM3 idealized simulations, and a subtropical Atlantic-based sea level pressure (SLP) anomaly with a maximum over the Gulf of Mexico. The idealized simulations demonstrate that a warm Pacific and/or a cold Atlantic are influential over regional hydroclimate features including the monthly preference for maximum GPLLJ and precipitation in the seasonal cycle. Furthermore, it appears that the regional expression of globally derived SST variability is important for generating an anomalous atmospheric low-level response of consequence to the GPLLJ, especially when the SST anomaly is positioned over a regional maximum in climatological SST, and in this case the Western Hemisphere warm pool.

### 1. Introduction

The central United States is a hydroclimatically and economically sensitive region given its agricultural

---

\* Current affiliation: NOAA/Climate Prediction Center, Camp Springs, Maryland.

---

*Corresponding author address:* Dr. Scott J. Weaver, Climate Prediction Center, NOAA/NWS/NCEP, 5200 Auth Road, Rm. 605, Camp Springs, MD 20746.  
E-mail: scott.weaver@noaa.gov

prominence and significant warm season precipitation variability. The proximity of this region to the Rocky Mountains, Gulf of Mexico, and Atlantic and Pacific Oceans provide a unique combination of potential climate influences, including large-scale atmospheric circulation variations emanating over the adjoining ocean basins and local land–atmosphere interactions. As such, the central United States is prone to significant interannual variations in precipitation, highlighted most recently by the flooding during the spring of 2008.

Pacific and Atlantic sea surface temperature (SST) variability is widely reckoned to influence central U.S. precipitation variations on multiple time scales. Using an observationally based approach, Barlow et al. (2001) and Ting and Wang (1997) found both tropical and North Pacific SST anomalies to be influential on summertime precipitation variations over the United States. GCM experiments have also been used to diagnose the role of tropical SST forcing on central U.S. warm season precipitation. Bates et al. (2001) show that the 1993 pluvial over the Great Plains was related to tropical Pacific SST anomalies; however, no such conclusion was drawn for the 1988 drought. Decadal SST variability has also been implicated in forcing drought and pluvial over the United States (Schubert et al. 2004, 2008; Seager et al. 2005). Given the dominance of the ENSO signal in generating global-scale climate anomalies, Atlantic SST influences on North American hydroclimate have only recently begun to gain traction, especially in summer. Emerging evidence suggests a significant role for the Atlantic in generating intraseasonal-to-interannual warm season precipitation anomalies over the continental United States, including atmospheric North Atlantic Oscillation (NAO) variability (Ruiz-Barradas and Nigam 2005; Weaver and Nigam 2008; Weaver et al. 2009) and mean SST in the Atlantic warm pool region (Wang et al. 2007).

A vitally important mechanism for warm season central U.S. precipitation variability is the Great Plains low-level jet (GPLLJ). Precipitation variations are extremely sensitive to this dynamic low-level circulation feature (see Fig. 4 herein) (Helfand and Schubert 1995; Higgins et al. 1997b; Schubert et al. 1998). As such, fluctuations in the strength, placement, and timing of the GPLLJ exert profound influence on the regional hydroclimate of the central United States. Efforts to more fully understand GPLLJ variability have uncovered interesting links to the large-scale atmospheric circulation variations emanating from the adjoining ocean basins (Byerle and Paegle 2003; Ting and Wang 2006; Weaver and Nigam 2008; Weaver et al. 2009), thermal and inertial characteristics produced by North American topography (Holton 1967; Ting and Wang 2006; Wexler 1961), and land surface features (Bosilovich and Sun 1999). However, the extent to which recurring modes of SST variability impact the GPLLJ has yet to be clarified and is the primary goal of this study. Unraveling basin-scale SST links to such an influential driver of central U.S. precipitation variations facilitates a more robust understanding of the mechanisms (i.e., the pathway) through which SST anomalies generate warm season hydroclimate variability, a notably difficult season for hydroclimate prediction (Saha et al. 2006).

Recently a U.S. Climate Variability and Predictability (CLIVAR) Drought Working Group was established in

an effort to enhance the understanding and prediction of drought and pluvial from seasonal to decadal time scales (Schubert et al. 2009). The multiagency collaboration includes the National Aeronautics and Space Administration (NASA), National Oceanic and Atmospheric Administration/National Centers for Environmental Prediction (NOAA/NCEP), National Center for Atmospheric Research (NCAR), NOAA/Geophysical Fluid Dynamics Laboratory (GFDL), Columbia University, and many other government and university scientists. These modeling centers have completed identical idealized SST-forced runs using their respective AGCMs. These idealized simulations provide a unique resource for assessing SST impacts on North American regional hydroclimate features, including the GPLLJ, and are utilized here. Additional analyses using observationally constrained reanalysis systems and Atmospheric Model Intercomparison Project (AMIP)-style GCM simulations serve as a contextual reference for the idealized responses.

Section 2 describes the observational data and AMIP and idealized SST model simulations. Section 3 discusses the structure of the seasonal cycle of the GPLLJ and interannual variability of precipitation. Section 4 shows connections of the GPLLJ to SST variability and the large-scale circulation. Section 5 highlights results from the idealized SST experiments, while section 6 is left for the summary and discussion.

## 2. Datasets and methodology

Several observationally based datasets are used to establish GPLLJ linkages to SST and precipitation. Atmospheric fields are gleaned from the NCEP–NCAR reanalysis (Kalnay et al. 1996) and the North American Regional Reanalysis (NARR; Mesinger et al. 2006) on  $2.5^\circ \times 2.5^\circ$  and  $1^\circ \times 1^\circ$  latitude and longitude grids, respectively. The SST field is taken from the Hadley Centre Sea Ice and Sea Surface Temperature dataset (HadISST) on a  $5^\circ \times 2.5^\circ$  latitude longitude grid (Rayner et al. 2003), while the precipitation comes from the  $2.5^\circ$  latitude  $\times$   $2.0^\circ$  longitude gridded U.S.–Mexico precipitation dataset (<http://www.cpc.ncep.noaa.gov/products/precip/realtime/retro.shtml>). The coarser-resolution NCEP–NCAR reanalysis is used more prominently because of its longer time record (NARR begins in 1979, NCEP–NCAR in 1949), while the NARR is used to interpret GPLLJ connectivity to the Gulf of Mexico precipitation, which is unavailable in the U.S.–Mexico dataset. The NARR precipitation field exhibits remarkable consistency with precipitation observations, a result that apparently reflects the successful assimilation of precipitation observations in the NARR system (Mesinger et al. 2006).

The two U.S. CLIVAR Drought Working Group AGCMs used in this study are the Seasonal-to-Interannual Prediction Project (NSIPP1) [NASA/Global Modeling and Assimilation Office (GMAO)] and Community Climate Model, version 3 (CCM3) [NCAR/Lamont-Doherty Earth Observatory (LDEO)]. The NSIPP1 and CCM3 model resolutions are on a  $3.75^\circ \times 3.0^\circ$  and  $2.8^\circ \times 2.8^\circ$  latitude–longitude grids, respectively. These two modeling centers provided a complete suite of idealized SST-forced simulations and 15-member (NSIPP1) and 16-member (CCM3) ensembles of AMIP-style runs. The presence of multiple ensemble members over the duration of the NCEP–NCAR reanalysis makes these models the best choice for this study, as the ensemble averages will enable the SST response to be more fully characterized. The NSIPP1 model formulation and its climate are described in Bacmeister et al. (2000), while the summer season predictability is established in Schubert et al. (2002). Details on the CCM3 model formulation can be found in Seager et al. (2005).

The idealized SST patterns are gleaned from a rotated EOF analysis of annual SST anomalies for the period 1901–2004 from the HadISST dataset (Rayner et al. 2003). The first three modes are retained and consist of a global trend pattern (explains 27.2% of the interannual variance), a pan-Pacific ENSO-like pattern (explains 20.5%), and an Atlantic pattern that resembles the Atlantic multidecadal oscillation (AMO) (explains 5.8%). Each GCM is forced with twice the standard deviation of the associated principal components (PCs) of all possible combinations and polarities (save the global trend, which is forced with 1 standard deviation) of SST variability on top of a monthly varying climatology for 50 years. Schubert et al. (2009) provide further details about the SST forcing and experimental design. The extreme forcing magnitude is meant to extract subtle linkages of SST variability to U.S. climate and should be taken into account when interpreting the results. Given our interest in assessing the relative contributions of the Pacific and Atlantic Oceans, we focus here on modes 2 (Pacific) and 3 (Atlantic). Table 1 adopted from Schubert et al. (2009) displays the abbreviations for the various SST forcing combinations used in the remainder of this study. For example the abbreviation denoting a combination of a warm Pacific and cold Atlantic is PwAc.

Much of the regional analysis is geographically focused on areas exhibiting interesting warm season variability in Great Plains precipitation and the GPLLJ (defined as the meridional winds at 925 hPa), which is maximum in the latitude and longitude bands of  $35^\circ$ – $45^\circ$ N,  $100^\circ$ – $90^\circ$ W and  $25^\circ$ – $35^\circ$ N,  $100^\circ$ – $95^\circ$ W, respectively (Ruiz-Barradas and Nigam 2005; Weaver and Nigam 2008; also see figures herein). As such these areas are

TABLE 1. The different combinations of the Pacific and Atlantic SST anomaly patterns used to force the GCMs. Here  $w$  refers to the warm phase of the pattern (with a 2 standard deviation weight) and  $c$  refers to the cold phase (with a 2 standard deviation weight). Also,  $n$  denotes neutral, indicating that the pattern has zero weight. In particular, the PnAn experiment denotes the control run forced with the annually varying climatological SST. Table adopted from Schubert et al. (2009).

	Warm Atlantic	Neutral Atlantic	Cold Atlantic
Warm Pacific	PwAw	PwAn	PwAc
Neutral Pacific	PnAw	PnAn	PnAc
Cold Pacific	PcAw	PcAn	PcAc

used to define the precipitation and GPLLJ indices. We note that modest shifts or expansion of these areas produced a negligible impact on the results.

In calculating climatological fields and their anomalies (i.e., departures from the climatology) the base period of 1949–2002 is used for the observational and AMIP-simulated analysis except where the NARR is employed because of its shorter record, beginning in 1979. For the idealized simulations 50-yr averages are used to calculate the mean state and the first year is discarded as the spinup period. The mean seasonal cycles are calculated as the 50-yr monthly climatology and standard deviation calculations are the 3-month mean of the monthly standard deviations.

### 3. GPLLJ and precipitation structure

#### a. Seasonal cycle

Figure 1 shows the seasonal cycle of the monthly mean GPLLJ in the NCEP–NCAR (solid), NARR (dashed), and U.S.–Mexico precipitation (dotted). The mean GPLLJ evolution is characterized by a spring intensification reaching a maximum of  $\sim 5.5 \text{ m s}^{-1}$  in June (NCEP) or July (NARR) and decaying throughout late summer. The seasonal cycle of mean precipitation is similar to the GPLLJ in terms of the spring intensification with a maximum of  $\sim 3.5 \text{ mm day}^{-1}$ ; however, the decay during late summer is less precipitous. The subtle differences in the GPLLJ among the NCEP–NCAR and NARR reanalyses are apparently not due to the time period differences (i.e., 1949–2002 for NCEP–NCAR and 1979–2002 for NARR), as restricting the calculation to the shorter NARR period still highlighted these differences.

#### b. Interannual variability

The seasonality of the interannual variability of precipitation is examined here by inspection of the standard deviation of precipitation from the U.S.–Mexico dataset for the April–June (AMJ) and July–September (JAS)

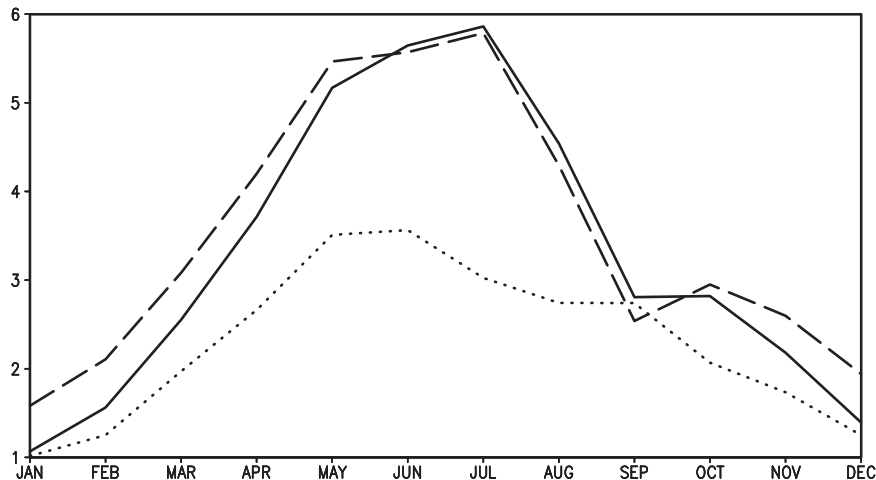


FIG. 1. Seasonal cycle of the GPLLJ in the NCEP (solid) and NARR (dashed) reanalyses and precipitation (dotted) in the U.S.-Mexico dataset. The GPLLJ is the area averaged meridional winds in the  $25^{\circ}$ - $35^{\circ}$ N,  $100^{\circ}$ - $95^{\circ}$ W box, while precipitation is area averaged in the  $35^{\circ}$ - $45^{\circ}$ N,  $100^{\circ}$ - $90^{\circ}$ W box. Precipitation is in  $\text{mm day}^{-1}$  and the GPLLJ is in  $\text{m s}^{-1}$ .

seasons during 1949–2002 (Fig. 2). These seasons mark the development and decay phases of the mean seasonal cycle of precipitation and the low-level jet (LLJ) over the Great Plains (Fig. 1). During AMJ the interannual variability of precipitation is strongest over the Gulf Coast states much like in the winter pattern of precipitation variability, that is, the coherent large-scale eastern two-thirds U.S. precipitation footprint. Summertime JAS precipitation variability is stronger than in AMJ over the Great Plains, with a maximum of  $1.8 \text{ mm day}^{-1}$ , and exhibits a more focused regional pattern. The East and Gulf Coasts of the United States and the North American monsoon (NAM) region highlight other interesting areas of precipitation variability.

#### 4. Large-scale context

##### a. SST links

Many studies of the GPLLJ and related precipitation variability focus on the months during jet development [AMJ/May–July (MJJ)] or maximum [June–August (JJA)]. While the early warm season is important for central U.S. precipitation variability (Fig. 2), the influence of spring SST anomalies on central U.S. precipitation variations is unclear, especially for the role of the tropical Pacific (Bates et al. 2001; Schubert et al. 2008). In fact, two of the most devastating early summer pluvial episodes over the Great Plains in recent memory occurred during anomalously warm (1993) and cold (2008) tropical Pacific SST regimes.

Figure 3 shows the GPLLJ index (defined in section 2) correlations to SSTs during 1949–2002 for the AMJ (left column), MJJ (middle column), and JAS (right column)

seasons in the NCEP–NCAR reanalysis (upper), NSIPP1 AMIP ensemble mean (middle), and CCM3 AMIP ensemble mean (lower), thus highlighting the seasonality of interannual variability. In the observations the correlations are quite weak during MJJ (save northwest Pacific) and JJA (not shown); however, they are considerably stronger during AMJ and JAS and reflect the importance of the Pacific in influencing GPLLJ anomalies during the time of development and decay in the mean seasonal cycle. During AMJ there is some agreement among the observed and ensemble mean simulations, however, in the Atlantic it is the NSIPP1 that is more like observations. The Pacific ensemble mean model simulations reflect the ambiguity in the GPLLJ–SST correlations during MJJ with the NSIPP1 displaying no coherent pattern and CCM3 showing a cold tropical Pacific, while in the Atlantic the simulations exhibit robust correlations regardless of the season. During JAS both the observed and simulated correlations are stronger in magnitude and exhibit a consistent pattern in the Pacific. The Atlantic correlations, while stronger than in AMJ or MJJ, are westward shifted in the simulations as compared to the observations, highlighting some differences over the Caribbean Sea and Gulf of Mexico. Overall the JAS SST correlations to the GPLLJ in observations and ensemble mean simulations are more coherent despite some regional structural differences. These SST patterns suggest that global-scale SST variability has the potential to impact GPLLJ variations during late summer.

The correlations of the seasonal mean GPLLJ index and SST in the NSIPP1 and CCM3 simulations (Fig. 3) are based on a multiple-member ensemble mean. It is not guaranteed that all ensemble members will exhibit

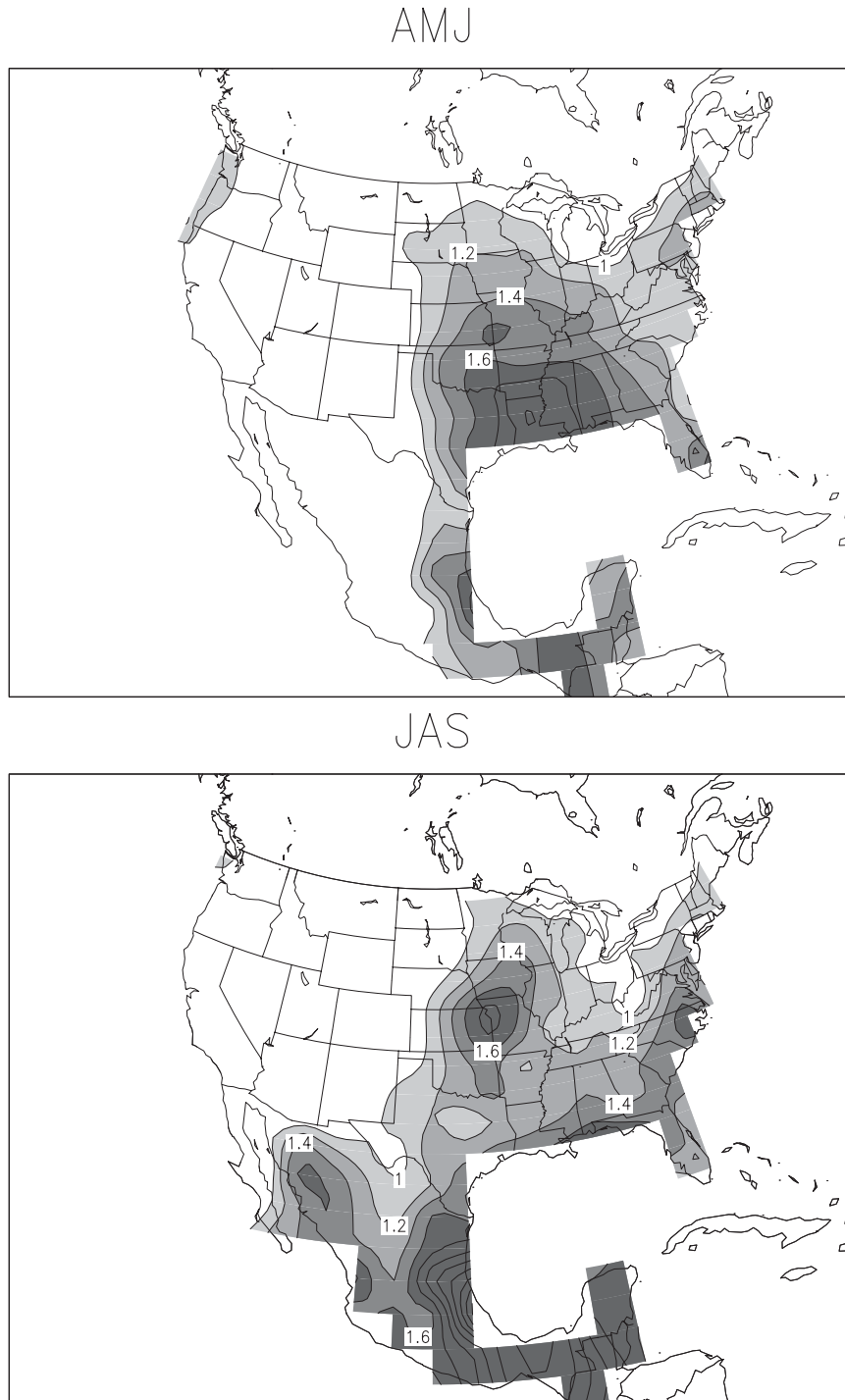


FIG. 2. The standard deviation of U.S.–Mexico precipitation for the period 1949–2002 during (top) AMJ and (bottom) JAS. Precipitation standard deviation greater than  $1 \text{ mm day}^{-1}$  is contoured at  $0.2 \text{ mm day}^{-1}$  intervals.

similar correlation structures. As an example, Fig. 4 shows the seasonal mean JAS GPLLJ index correlations to SST for 1949–2002 for all 15 members of the NSIPP1 AMIP simulations. While the correlation structure

varies between the ensemble members, nearly all runs show positive values through the eastern and central Pacific flanked by negative correlations to the north and south. The negative correlations in the North Atlantic

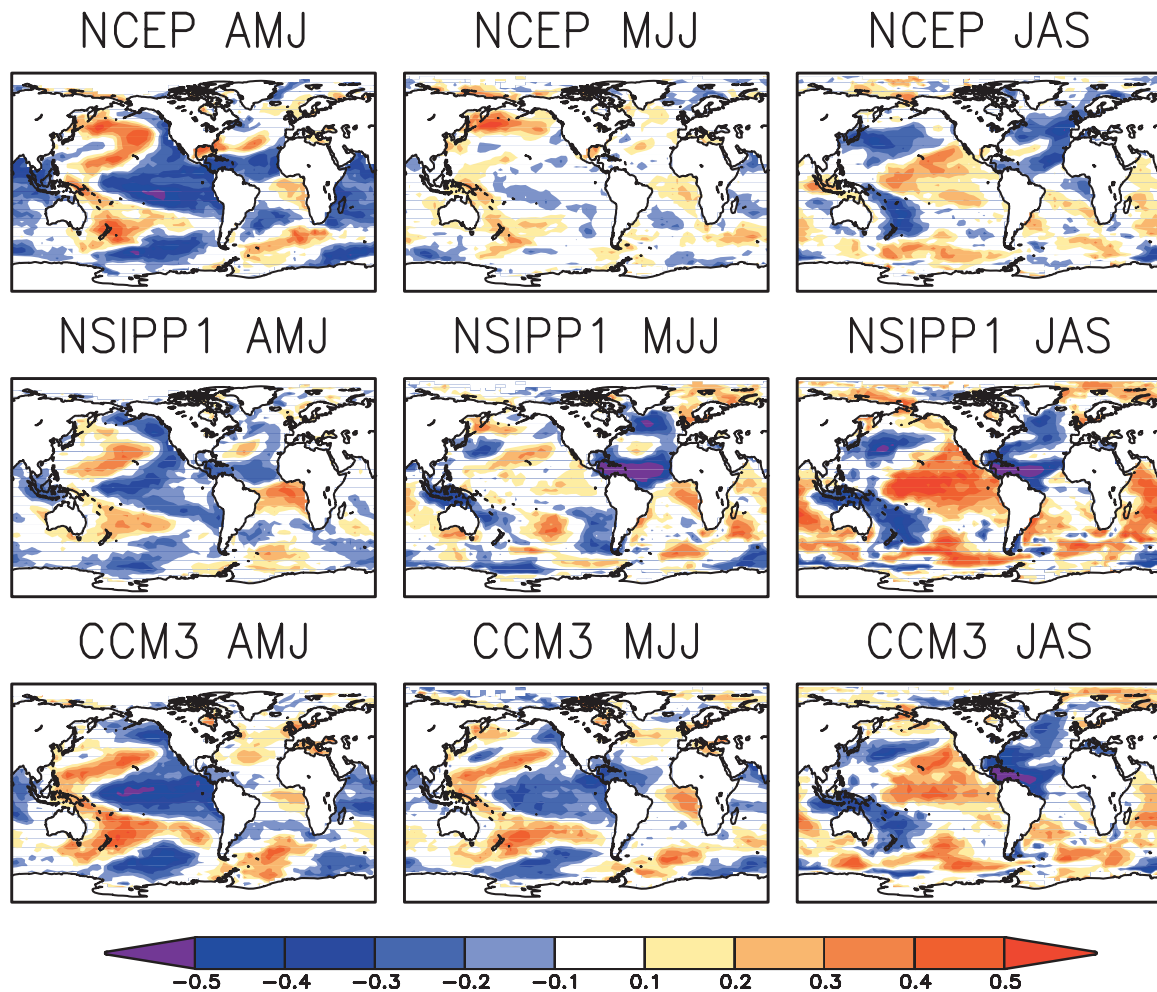


FIG. 3. The correlation of the seasonal mean GPLLJ index with SSTs for (left) AMJ, (center) MJJ, and (right) JAS during 1949–2002. (top) The GPLLJ indices derived from the NCEP–NCAR reanalysis; the ensemble mean simulated correlations for (middle) NSIPP1 and (bottom) CCM3. The shading interval is 0.1.

show more consistency in magnitude and structure among the ensemble members.

#### b. GPLLJ and precipitation variability

The coherent correlations of the GPLLJ index to SSTs and the stronger and more regionally focused Great Plains precipitation variability during JAS (Fig. 2) suggest that this season is important for diagnosing SST influences on the GPLLJ and its precipitation impacts— notwithstanding the potential NAM influence in reducing Great Plains precipitation in the mean seasonal cycle and interannual variability (Higgins et al. 1997a, 1998). Furthermore, the monthly correlation of the Great Plains precipitation and LLJ indices during JAS (AMJ) is 0.62 (0.36). As such we will focus our attention on the JAS months in the remaining analysis.

Figure 5 shows the regressions of the seasonal mean JAS GPLLJ index on 925-hPa meridional winds (con-

toured) and precipitation (shaded) in the NARR (upper left), the U.S.–Mexico (upper right), CCM3 (lower left), and NSIPP1 (lower right). The placement of the NARR and U.S.–Mexico precipitation regressions in the Midwest and southeastern United States are consistent with those of the standard deviation of JAS precipitation in the bottom panel of Fig. 2, although the magnitude is approximately one-half. These regression patterns suggest that GPLLJ and precipitation variations during JAS are related to a coherent large-scale circulation pattern that also has implications for southeastern U.S. precipitation variability. An interesting difference between the NARR and U.S.–Mexico precipitation variability is the lack of a North American monsoon precipitation anomaly in the NARR representation, which is not seen in the U.S.–Mexico depiction. The cause is most likely related to reanalysis/observing system deficiencies as similar pattern differences emerge when the NCEP/U.S.–Mexico

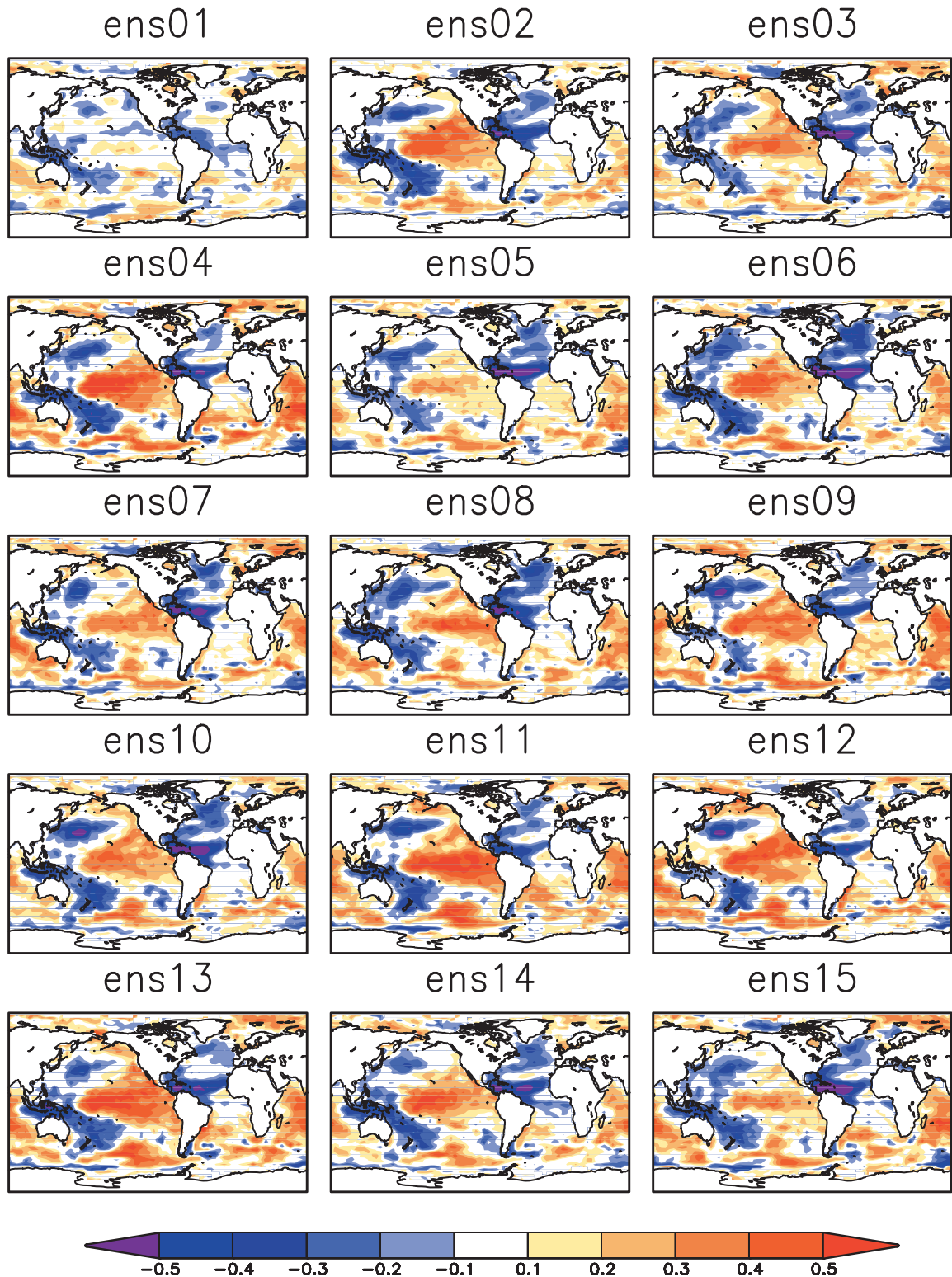


FIG. 4. The correlation of the seasonal mean GPLLJ index anomalies with SSTs for the 15 NSIPP1 AMIP ensemble members during JAS for 1949–2002. Correlations are shaded beginning at  $\pm 0.1$  and the shading interval is 0.1.

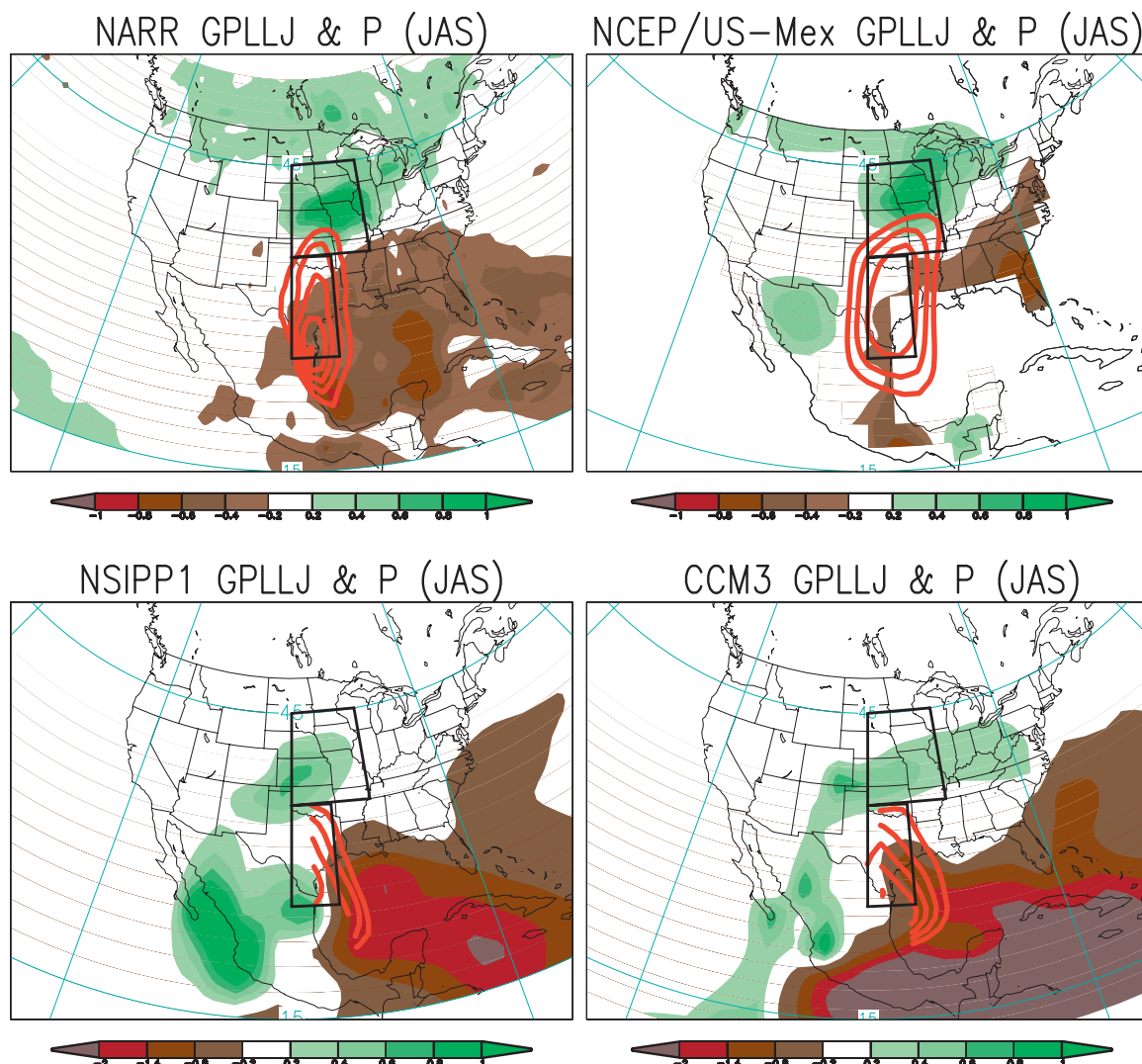


FIG. 5. Regression of the seasonal mean (JAS) GPLLJ index anomalies on precipitation (shaded) and 925-hPa meridional winds (contoured) for (top left) 1979–2002 in NARR, (top right) 1949–2002 in NCEP/U.S.–Mexico, (bottom left) CCM3 AMIP ensemble mean, and (bottom right) NSIPP1 AMIP ensemble mean. The meridional wind regressions are contoured at  $0.2 \text{ m s}^{-1}$  intervals while precipitation is shaded. Note the varying shading intervals for negative precipitation values in the observed and simulated panels.

regression is restricted to the shorter NARR time period (i.e., 1979–2002). It is widely known that during the JAS period the North American monsoon is an important climatic feature over the United States and is typically characterized by an out-of-phase relationship between precipitation over the Great Plains and NAM region, (Barlow et al. 1998; Berbery and Fox-Rabinovitz 2003; Higgins et al. 1997a, 1998, 1999). However, there is some evidence that this phase relationship emerged only after 1962 (Kim 2002), further confounding its absence in the more recent (1979–2002) NARR record.

The AMIP ensemble mean GPLLJ-related precipitation anomaly is shifted to the south and west in both the NSIPP1 and CCM3 models when compared to observa-

tions. The Great Plains precipitation anomaly is weaker than its observed counterpart by about one-third, while the negative precipitation anomaly (note the shading interval) over the Caribbean Sea and Gulf of Mexico is nearly double! Both NSIPP1 and CCM3 also show an anomalous North American monsoon precipitation pattern, with the NSIPP1 being significantly stronger, perhaps indicating the inability to capture the negative phase relationship between the Great Plains and North American monsoon characteristics in the interannual variability.

### c. Large-scale circulation variability

The global-scale SST pattern during GPLLJ strengthening suggests that large-scale atmospheric circulation

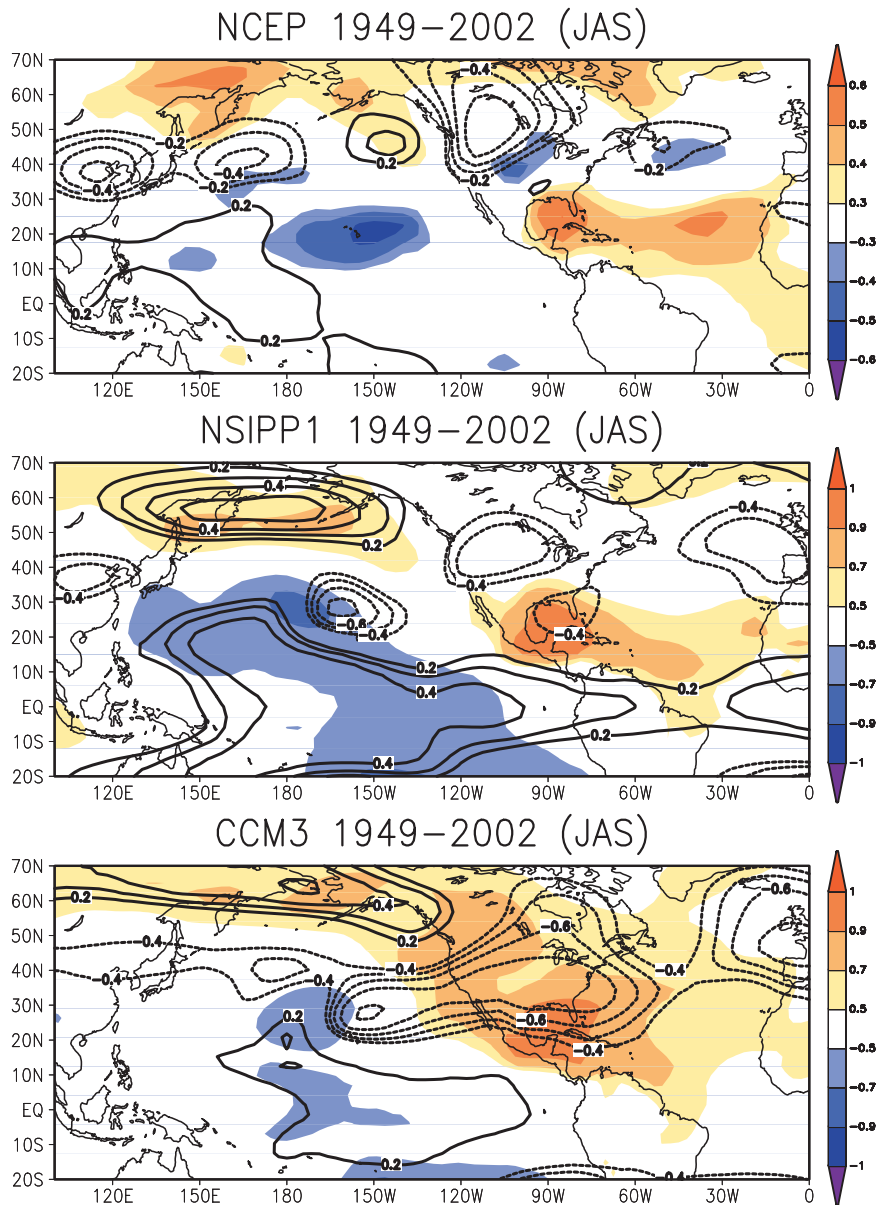


FIG. 6. Correlation of the seasonal mean (JAS) GPLLJ index anomalies with SLP (shaded) and 200-hPa height (contoured) in the (top) NCEP reanalysis, (middle) NSIPP1 AMIP ensemble mean, and (bottom) CCM3 AMIP ensemble mean for 1949–2002. The 200-hPa heights are contoured at 0.2 intervals. The SLP is shaded at 0.1 intervals beginning at  $\pm 0.3$  in the observed panel shading and contoured at 0.2 beginning at  $\pm 0.5$  in the model panels.

variability may be related to regional GPLLJ variations. To investigate this we perform correlations of the seasonal mean JAS GPLLJ index to 200-hPa height and sea level pressure (SLP) anomalies during 1949–2002 in the NCEP–NCAR reanalysis and NSIPP1 and CCM3 ensemble mean AMIP simulations (Fig. 6).

The late summer GPLLJ variability is associated with an apparent upper-level wave train emanating from the east Asia/tropical west Pacific region. Similar upper-

level patterns have been noted before in the context of North American precipitation variability (Bell and Janowiak 1995; Ding and Wang 2005) and more recently with respect to observed springtime GPLLJ variability (Weaver and Nigam 2008). The models are challenged in reproducing this pan-Pacific feature in the ensemble mean, although both place negative height anomalies over North America. The NSIPP1 has a much stronger response in the tropical upper-level height anomalies

in both magnitude and coverage. Despite some differences in the upper-level heights the SLP field exhibits more consistency among the models and observations, especially over the Atlantic sector. The stronger magnitude modeled correlations (note the higher shading threshold) are likely due to the multiple ensemble averaging of the simulations, which highlights the SST-forced component of the variability. In general the NSIPP1 AMIP simulation reproduces more closely the observed SLP anomaly than in the CCM3. While the CCM3 does place anomalous SLP over the Gulf of Mexico, it is part of a large-scale positive anomaly over the North American continent not seen in the NCEP or NSIPP correlations.

## 5. Idealized SST

### a. SST patterns

The previous sections established the link between the GPLLJ, its related precipitation, and basin-scale SST and atmospheric circulation patterns in observations and AMIP climate model simulations. In this section we turn our attention to characterizing the influence of Atlantic and Pacific SST modes in generating GPLLJ variability. This phase of the analysis will enable the separation of Atlantic and Pacific basin influences to understand their role in generating GPLLJ variability during summer. The SST forcing patterns are derived from a rotated EOF (REOF) analysis of annual mean SST for 1901–2004 and are described in more detail in section 2 and in Schubert et al. (2009).

The positive (warm) phases of the patterns used in this analysis (modes 2 and 3) are shown in Fig. 7. The Pacific pattern (REOF 2) clearly shows the presence of the ENSO mode of variability in the tropical Pacific. Pacific decadal SST structure is also evident given the meridional broadening of the tropical SST anomaly and west coast of North America focus. The Atlantic pattern (REOF 3) is similar to the SST footprint associated with the AMO and NAO. These SST patterns are similar in many respects to the SST correlations associated with the GPLLJ variability (Fig. 3). The following analysis will examine the responses of the GPLLJ and large-scale circulation features to various polarities and combinations of these idealized SST patterns in the NSIPP1 and CCM3 AGCMs.

### b. Seasonal cycle of GPLLJ and precipitation

To assess the impact of the various SST forcings on the central U.S. climate in Figs. 8 and 9 we show the seasonal cycle of the GPLLJ (top panels) and precipitation (lower panels) in the NSIPP1 (Fig. 8) and the CCM3 (Fig. 9). The colored lines denote the various idealized

SST forcing experiments (see inset key) and each panel contains the observed and AMIP counterpart highlighted by the black and blue lines, respectively. The mean seasonal cycle response is based on 50-yr monthly averages. When comparing the AMIP runs (blue lines) and observations (black lines) in Figs. 8 and 9 it is evident that both the NSIPP1 and CCM3 underestimate the seasonal cycle of the 925-hPa meridional winds throughout the year (although NSIPP1 matches exactly in the month of July) and are especially challenged in depicting the fall decay of the mean GPLLJ. In fact, both the NSIPP1 and CCM3 exhibit negative mean meridional winds during fall. The seasonal cycle of precipitation over the northern Great Plains is captured much better in the winter and spring seasons; however, it is overestimated (underestimated) during summer (fall).

A striking aspect of the GPLLJ in the idealized model simulations is the lack of sensitivity to the sign of the SST forcing during spring and the robust response during the summer and fall, especially in the NSIPP1, although it is possible that this is due to model systematic errors. Both models agree on the general aspect of GPLLJ response in summer, that being a warm Pacific and cold Atlantic (PwAc) strengthens the GPLLJ, while the opposite-signed SST anomalies (PcAw) weakens it. The contributions of the Pacific- and Atlantic-only runs [i.e., neutral Pacific/warm Atlantic (PnAw), neutral Pacific/cold Atlantic (PnAc), warm Pacific/neutral Atlantic (PwAn), and cold Pacific/neutral Atlantic (PcAn)] fall within the bounds of the most extreme SST forcing highlighting that in the simulations a cold (warm) Atlantic (Pacific) strengthens the GPLLJ while the opposite weakens it. There are also implications for the timing of the peak magnitude in the seasonal cycle with the PcAw exhibiting a maximum one month earlier than the PwAc scenario. This undoubtedly would have significant implications for the timing of peak moisture availability and dynamic low-level convergence in the central United States. The precipitation response exhibits similar characteristics; however, the degree of sensitivity to the prescribed SST is weaker than that seen in the GPLLJ response, which is not surprising as the GPLLJ and Great Plains precipitation do not necessarily exhibit a one-to-one correspondence.

An interesting aspect of the spring response in the CCM3 is the suggestion, although weak, that the same SST anomaly could have opposite impacts on the GPLLJ, however, not on precipitation. For instance the PcAw scenario produces the strongest (weakest) GPLLJ during the spring (summer) in the CCM3. On the other hand, the relative precipitation response is consistent throughout the spring and summer. This feature is not inconsistent with the observed nature of

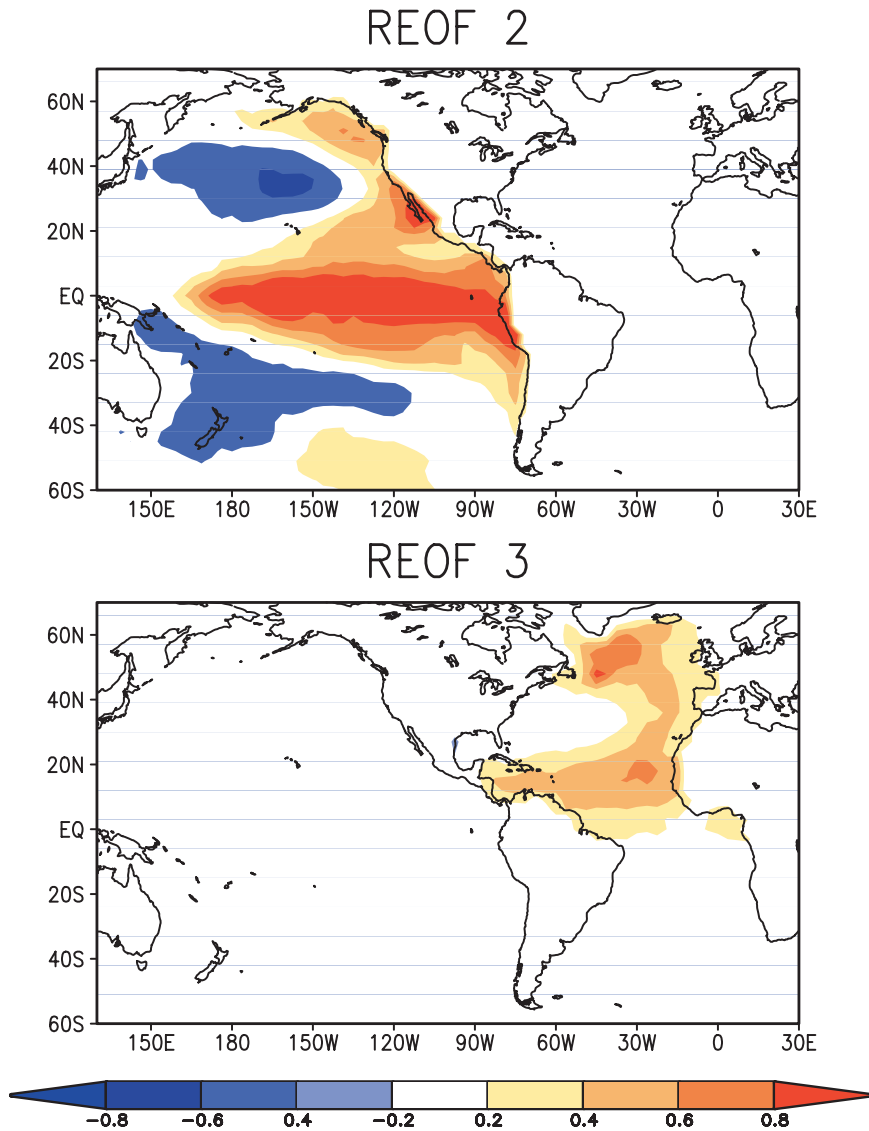


FIG. 7. SST forcing patterns for U.S. CLIVAR Drought Working Group AGCM experiments. The shading interval is 0.2. Only the positive polarity is shown.

the GPLLJ and precipitation where the spring correlations are weaker (i.e., 0.36 in AMJ and 0.62 in JAS).

### c. Regional and large-scale circulation

From the seasonal cycle and mean response of the GPLLJ and precipitation to idealized SST forcing patterns in two state-of-the-art climate model simulations, it appears that oppositely signed SST anomalies in the Atlantic and Pacific may be important for the GPLLJ and Great Plains precipitation. This precipitation response is also noted in Schubert et al. (2008). The idealized model simulations afford a unique opportunity to investigate the relative roles of the Atlantic and Pacific SST modes on the spatial structure of the GPLLJ and

precipitation over the central United States and the large-scale circulation. In the remaining sections the responses are expressed as differences in the 50-yr means.

Figure 10 shows the response of the GPLLJ and precipitation (upper panel, NSIPP-only; CCM3 is similar and is not shown) and large-scale circulation (middle, NSIPP1; lower, CCM3) under the warm Pacific and neutral Atlantic scenario. The upper panel shows that the GPLLJ and precipitation are markedly enhanced under the warm Pacific (i.e., PwAn–PcAn) scenario. The precipitation anomaly, while large, appears to be underestimated, given the magnitude of the GPLLJ strengthening. Both the NAM and Gulf of Mexico

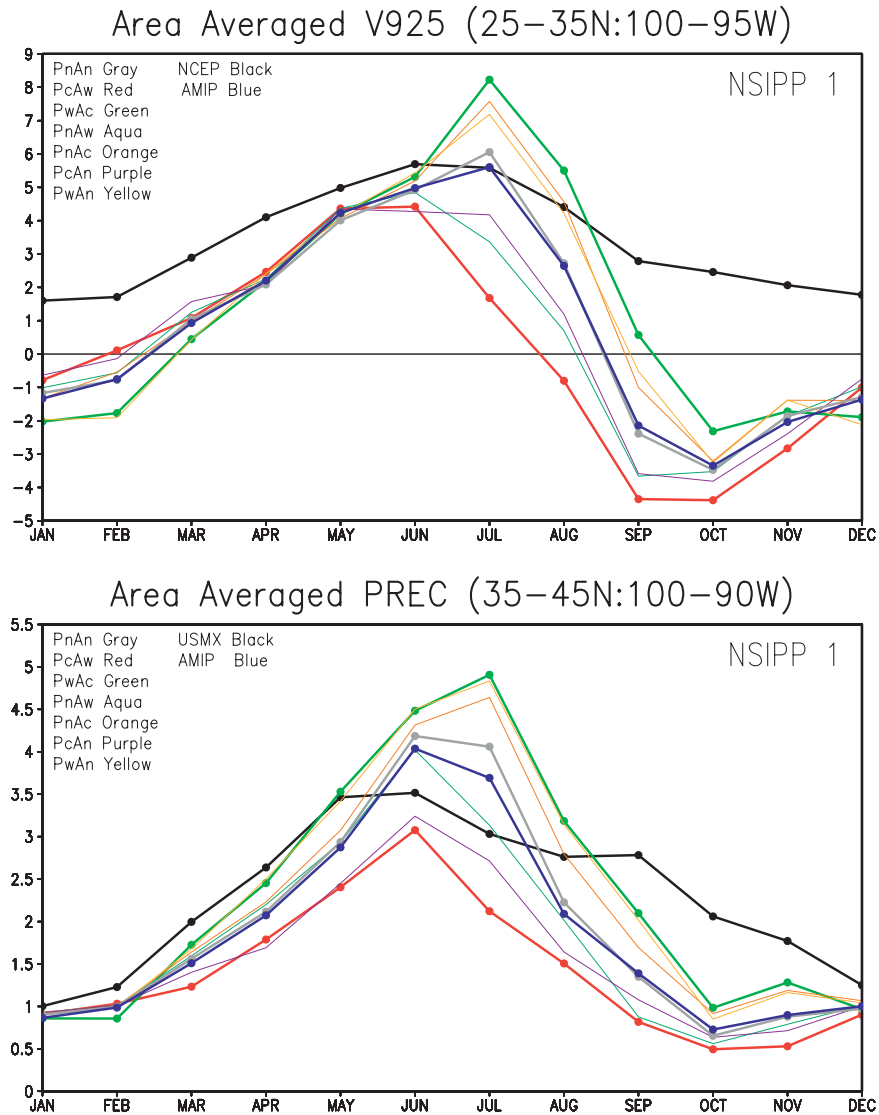


FIG. 8. Mean seasonal cycle of the (top) GPLLJ and (bottom) precipitation in the NSIPP1 idealized SST experiments. The GPLLJ is in  $\text{m s}^{-1}$  and the precipitation is in  $\text{mm day}^{-1}$ . Each panel includes a key to discern the origin of the data and polarity of the SST forcing.

precipitation responses are quite strong. The large-scale circulation response is characterized by a strong positive upper-level 200-hPa height anomaly over the tropical Pacific and a weaker negative anomaly over the northern tier of the United State in both models. The low-level SLP response is similar to the GPLLJ index correlation AMIP response in Fig. 6, with a strong focus in the Gulf of Mexico.

In the cold Atlantic scenario (Fig. 11) the GPLLJ response is similar to that of the warm Pacific; however, the precipitation anomaly is weaker. This model response is consistent with the AMIP simulations (Fig. 5) where the GPLLJ-related precipitation anomaly was weaker than

the observed. This is not surprising given the model precipitation dependence on physical parameterizations.

The cold Atlantic upper-level height response differs when compared to the warm Pacific counterpart. Both the NSIPP1 and CCM3 place negative height anomalies in a region encompassing the eastern subtropical Pacific and most of the Atlantic. The SLP response is quite similar in the CCM3 in both the warm Pacific (Fig. 10) and cold Atlantic (Fig. 11) scenarios. The NSIPP1, however, differs in the geographic extent and magnitude of the SLP anomaly between the warm Pacific and cold Atlantic scenarios. With a cold Atlantic, the SLP anomaly is stronger and more expansive, extending to the

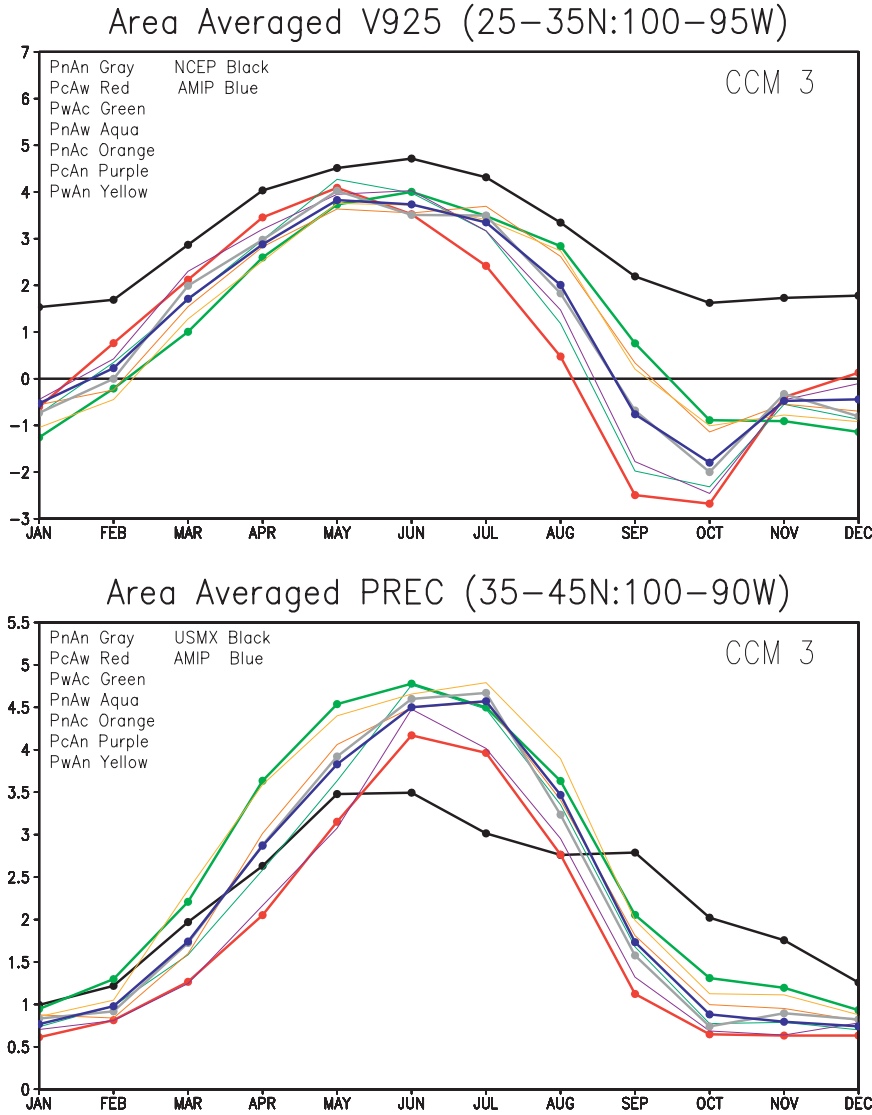


FIG. 9. Mean seasonal cycle of (top) the GPLLJ and (bottom) precipitation in the CCM3 idealized SST experiments. The GPLLJ is in  $m s^{-1}$  and the precipitation is in  $mm day^{-1}$ . Each panel includes a key to discern the origin of the data and polarity of the SST forcing.

African coast, and again with a Gulf of Mexico focus.<sup>1</sup> The mean GPLLJ and precipitation values are all significantly different from each other at the 1% level based on a *t* test.

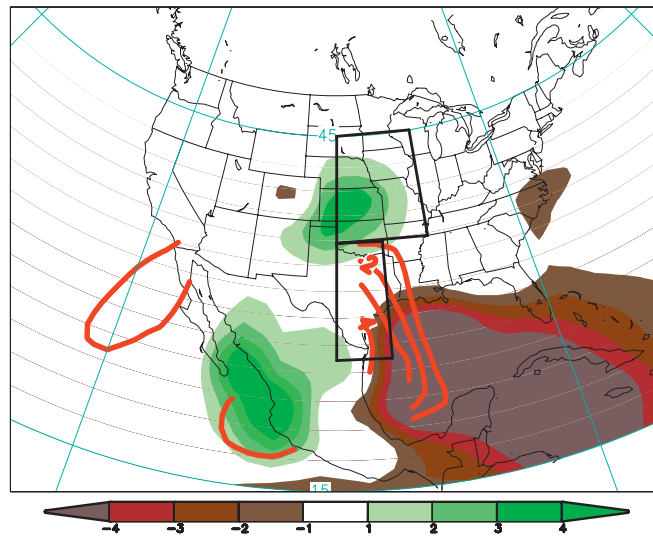
*d. Physical mechanisms*

The above analysis suggests the importance of SLP in the Gulf of Mexico and Caribbean region in modulating GPLLJ and precipitation variations over the central

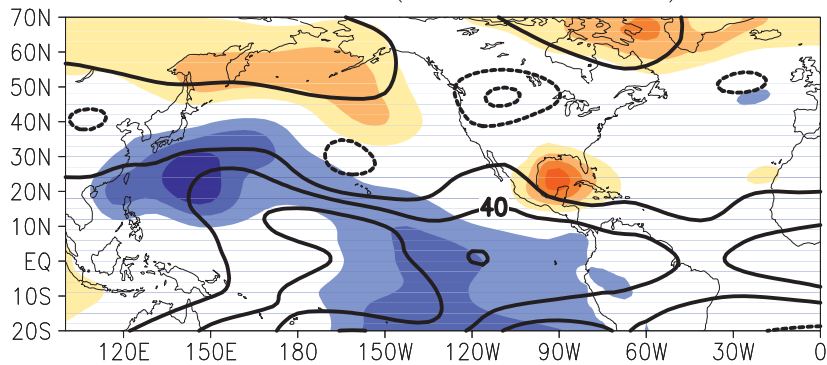
United States. To be sure, there are certainly contributions to North American precipitation variations by these large-scale SST anomalies from forced atmospheric responses emanating from remote regions (i.e., teleconnection responses; see Fig. 6 top panel). While the upper-level patterns in Figs. 10 and 11 hint at this mechanism, the strong response in Gulf of Mexico SLP is arguably a more enticing avenue of investigation, especially given its large magnitude. Large-scale Atlantic and Pacific SST variability, and in particular a warm Pacific/cold Atlantic, appears important in generating this regionally focused SLP anomaly, as the response to forcing from either basin shows a regional maximum in the SLP response. Furthermore, correlations of the

<sup>1</sup> An inspection of the most extreme response to the SST forcing patterns (i.e., PwAc–PcAw) is essentially a linear combination of the responses in Figs. 10 and 11.

## NSIPP1 (PwAn-PcAn)



## NSIPP1 (PwAn-PcAn)



## CCM3 (PwAn-PcAn)

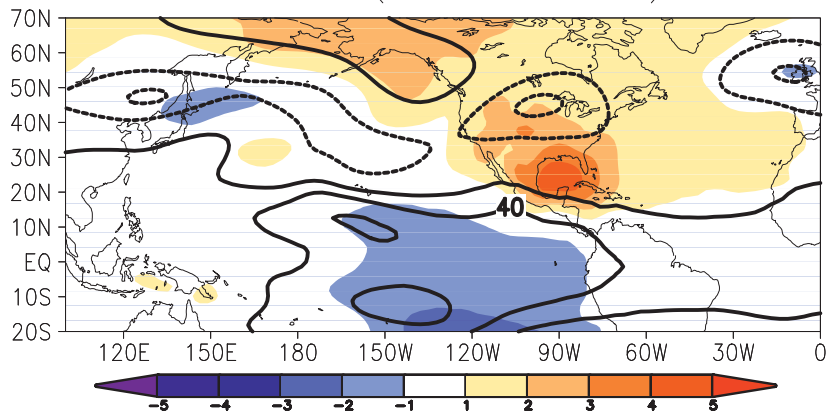


FIG. 10. JAS mean response to warm Pacific idealized SST expressed as the difference in the warm minus cold Pacific with the Atlantic neutral in the (top), (middle) NSIPP1 AGCM and (bottom) CCM3. NSIPP1 GPLLJ and precipitation (top) are contoured and shaded at  $1 \text{ m s}^{-1}$  and  $1 \text{ mm day}^{-1}$ , respectively. In (middle) and (bottom), SLP (shaded) and 200-hPa height (contoured) responses are at 20 m and 1 hPa, respectively.

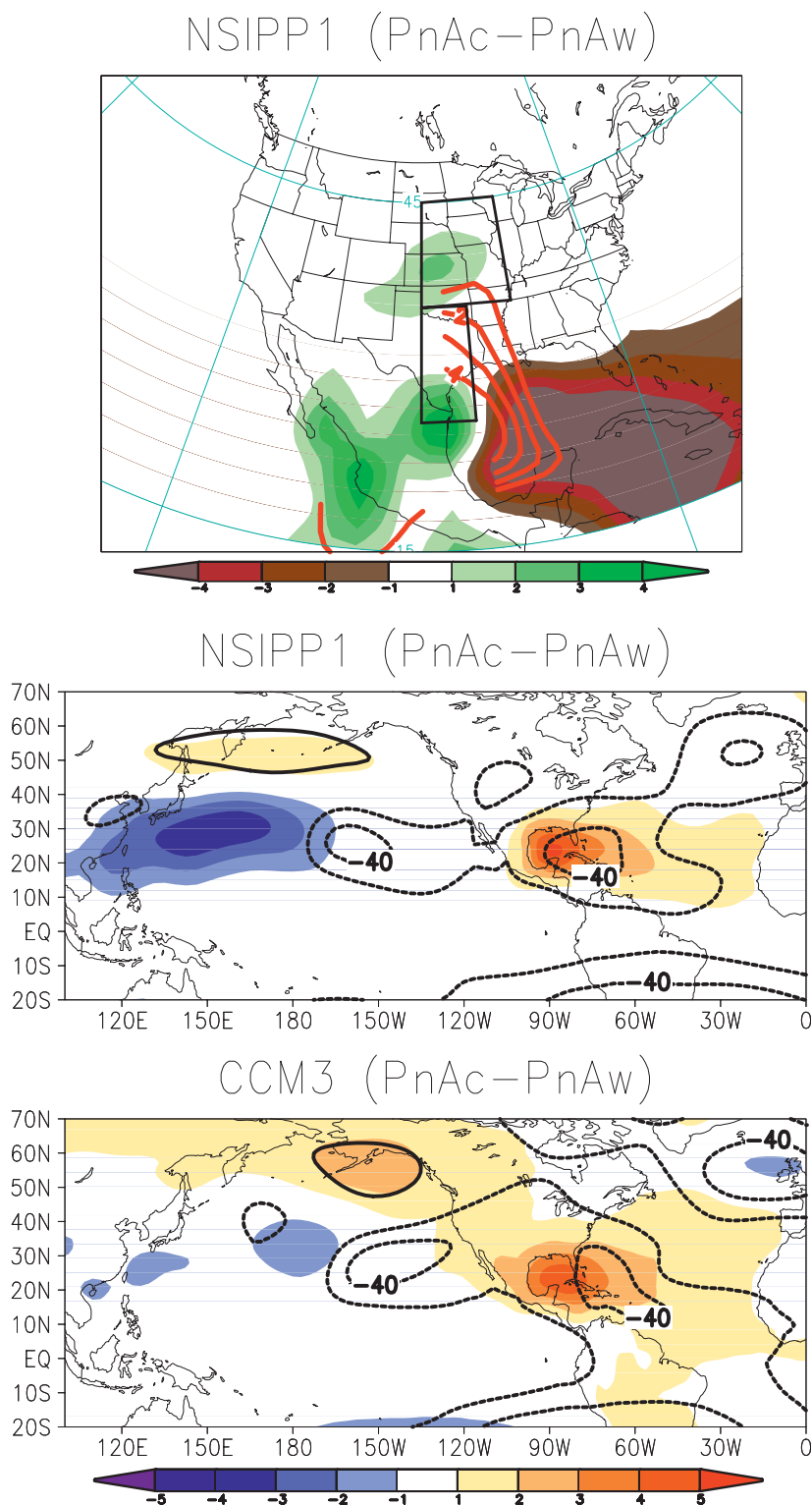


FIG. 11. JAS mean response to cold Atlantic idealized SST expressed as the difference in the cold minus warm Atlantic with the Pacific neutral in the (top), (middle) NSIPP1 AGCM and (bottom) CCM3. NSIPP1 GPLLJ and precipitation (top) are contoured and shaded at  $1 \text{ m s}^{-1}$  and shaded at  $1 \text{ mm day}^{-1}$ , respectively. In (middle) and (bottom), SLP (shaded) and 200-hPa height (contoured) responses are at 20 m and 1 hPa, respectively.

observed and AMIP ensemble mean GPLLJ index with SLP during JAS of 1949–2002 also establish this link (Fig. 6).

Figure 12 shows the SST EOF forcing patterns (shaded) and the JAS climatological SST (contoured) (top panel) and the precipitation (shaded) and SLP (contoured) (bottom panel) response from the difference between PwAc and PcAw in the Western Hemisphere warm pool region. This region encompasses the extreme eastern Pacific, Gulf of Mexico, and Caribbean Sea. It is quite apparent that even in globally derived SST variability there exist significant meridional and zonal SST gradients in this area. The close proximity of the SLP response to the SST gradients suggests that regional circulation features related to the SST gradient may be important, especially since no regional SST anomaly exists over the Gulf of Mexico, thus providing marginal direct thermodynamic forcing to the SLP anomaly. The maximum precipitation (lower panel) anomalies are located over the area of maximum warm SST climatology as outlined by the 28°C isotherm, suggesting that the model response is to generate precipitation anomalies where the area of warmest SST is perturbed.

Given that the idealized SST patterns and in particular a warm Pacific and cold Atlantic appears important in generating a regional SLP anomaly that can strengthen the GPLLJ and central U.S. precipitation it is of interest to analyze the regional moisture flux response. Figure 13 shows the column-integrated (1000–200 hPa) moisture fluxes (arrows) and their convergence (shaded) for the PwAn–PcAn (upper) and the PnAc–PnAw (lower) scenarios. The moisture fluxes and their convergences are remarkably similar in the two idealized responses and are generally collocated with the precipitation anomalies (Figs. 10, 11, and 12). The only appreciable difference is that there is weak anomalous moisture flux over the Pacific west of 105°W in the PwAn–PcAn.

The similarity of the response suggests that enhancing the interbasin SST gradient by either warming the Pacific or cooling the Atlantic will lead to a similar precipitation anomaly over the warmest climatological SST and an enhancement of the easterly moisture fluxes (i.e., easterlies) between 5° and 20°N. The placement of the SLP anomaly to the northwest of the Atlantic precipitation (i.e., latent heating) anomaly is consistent with the classic regional atmospheric response to an off-equatorial heating (or cooling) anomaly (Gill 1980).

## 6. Summary and discussion

The Great Plains of North America exhibit significant precipitation variations during the warm season. Recent studies have linked global SST variability to central U.S.

precipitation fluctuations on multiple time scales. In this study the role of SST variability and its link to the GPLLJ is investigated given the jet's influence on Great Plains summertime precipitation variability.

Interannual variability of the GPLLJ is shown to be linked to global-scale SST variability during the summer (JAS) over the period 1949–2002 in observationally constrained reanalysis (NCEP–NCAR) and NSIPP1 and CCM3 AMIP climate model simulations. An interesting finding is the seasonal dependence of the link between SST and GPLLJ variability. The strongest correlations of the GPLLJ index to SST are found during the AMJ and JAS seasons, with MJJ and JJA being weaker. However, given the stronger precipitation variability and higher correlation of the GPLLJ and precipitation indices during JAS (0.62) when compared to AMJ (0.36) we focus on the JAS “season.”

By applying regressions of the GPLLJ index anomalies it is found that NSIPP1 and CCM3 ensemble mean AMIP simulations produce some characteristics of the observed GPLLJ-related precipitation variability over the United States, Mexico, and the Gulf of Mexico. However, the AMIP response gives weaker precipitation anomalies over the Great Plains and stronger ones over the west coast of Mexico, Gulf of Mexico, and Caribbean Sea as compared to those in observationally constrained data. Correlations of the GPLLJ with SLP and 200-hPa heights in the NCEP–NCAR reanalysis reveal that the GPLLJ is related to a large-scale pan-Pacific wave train pattern and an Atlantic-based subtropical SLP anomaly. The CCM3 and NSIPP1 AMIP ensemble mean correlations show varying 200-hPa height anomaly structures; however, they agree on the location of the SLP anomaly, especially the maximum over the Gulf of Mexico.

The seasonal cycle of the GPLLJ and northern Great Plains precipitation in idealized SST climate model simulations indicates that a warm Pacific and cold Atlantic enhances the strength of the GPLLJ and northern Great Plains precipitation. Additionally, the timing and sensitivity of the seasonal cycle of the GPLLJ and precipitation is impacted under this idealized forcing. In particular the GPLLJ response is less sensitive to the sign of the spring SST anomaly as compared to summer, where the spread is large, and the peak timing of the GPLLJ is a month earlier (June) in the PcAw case than the PwAc (July), especially in the NSIPP1.

The idealized simulations offer an opportunity to also examine the spatial structure of regional GPLLJ, precipitation, and SLP anomalies during JAS and the relative roles of the Pacific and Atlantic SSTs by examining the model responses to forcing from one basin while keeping the other neutral. Interestingly, the low-level

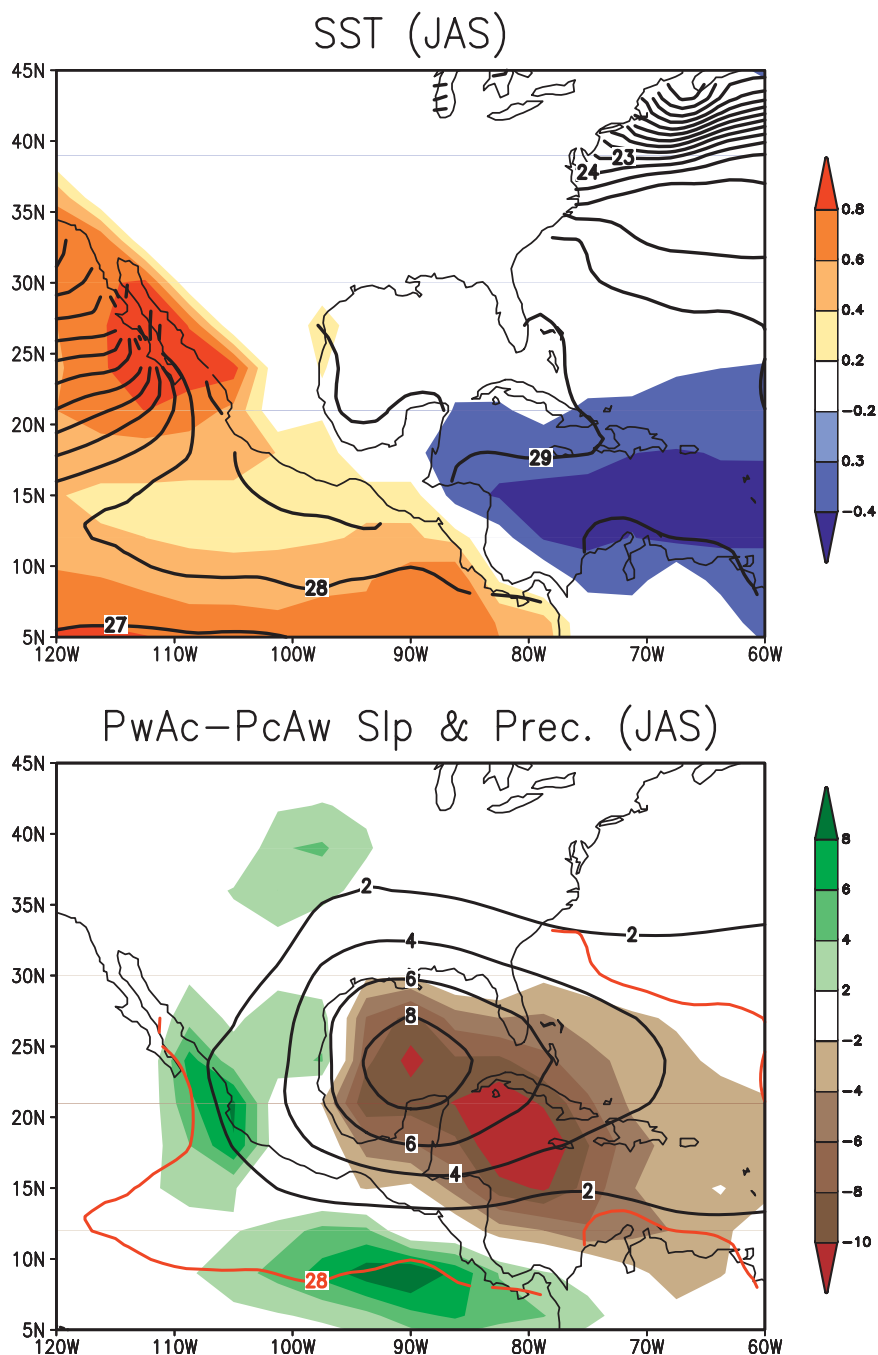


FIG. 12. (top) Regional expression of climatological SST (contoured) EOFs 2 (Pacific) and 3 (Atlantic) (shaded) and (bottom) SLP (contoured) and precipitation (shaded) for the PwAc-PcAw idealized SST scenario in NSIPP1. SLP and precipitation is contoured at 2 hPa and 2 mm day<sup>-1</sup> intervals, respectively. The 28°C isotherm is contoured in red to highlight the Western Hemisphere warm pool.

circulation (i.e., the GPLLJ and SLP) and precipitation were similar in the model simulations regardless of the prescribed forcing (i.e., warm Pacific/neutral Atlantic or cold Atlantic/neutral Pacific) and place a maximum in

SLP over the Gulf of Mexico. The intermodel depiction of this feature is generally consistent, although the CCM3 casts the Gulf of Mexico SLP maximum as part of a large-scale SLP anomaly over North America, while

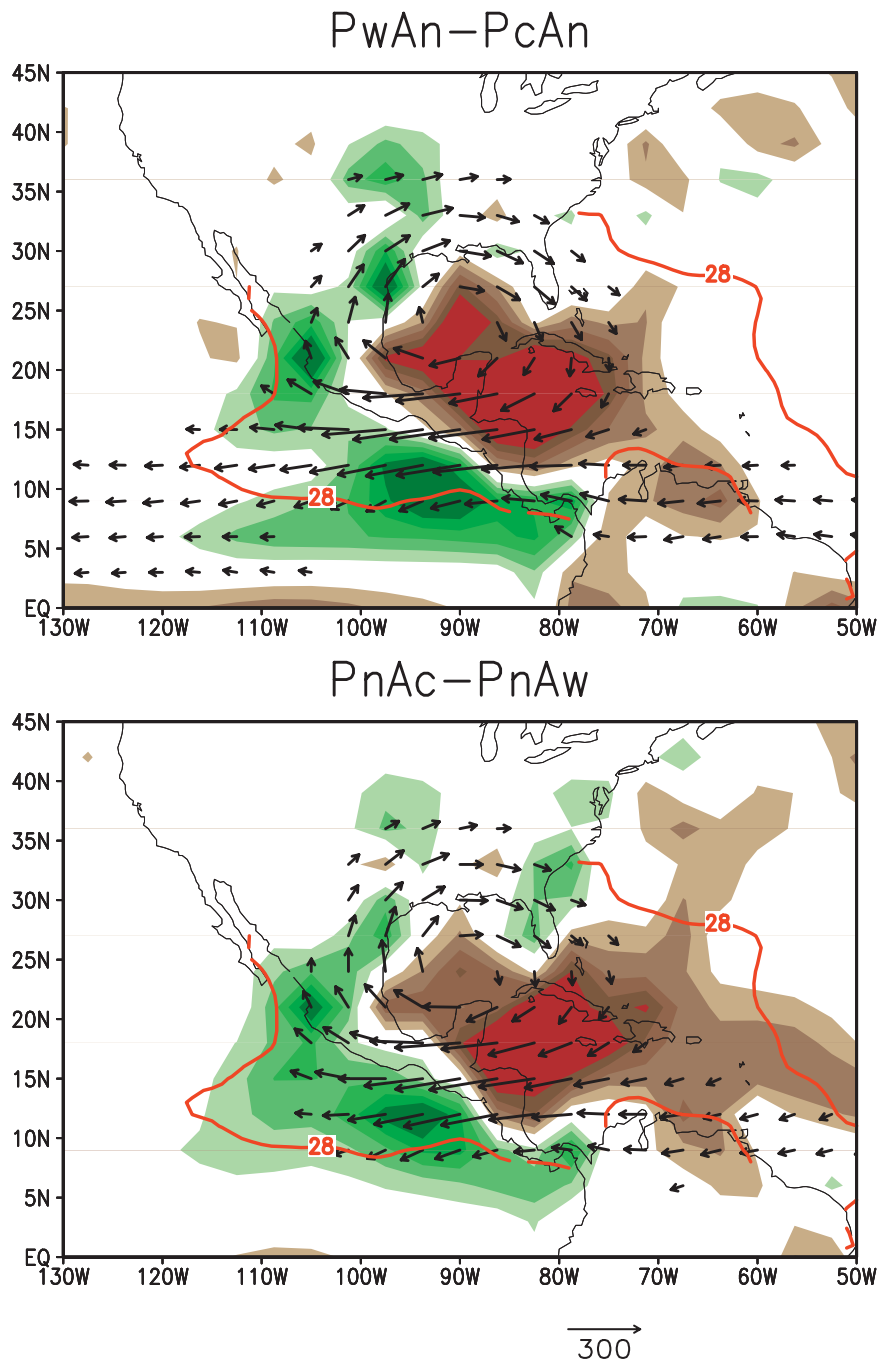


FIG. 13. Vertically integrated 1000–200 hPa moisture flux (arrows) and convergence (shaded) for the difference between (top) a warm minus cold Pacific and (bottom) a cold minus warm Atlantic during JAS. The reference moisture flux vector is  $300 \text{ kg m}^{-1} \text{ s}^{-1}$  and the moisture flux convergence (divergence) is shaded green (brown) at  $1 \text{ mm day}^{-1}$  intervals. The  $28^\circ\text{C}$  isotherm is contoured in red to highlight the Western Hemisphere warm pool.

the NSIPP1 SLP response remains highly localized. The upper-level 200-hPa height response varies among the different SST forcing with the Pacific exhibiting a more global reach, while the Atlantic is more regionally con-

finied. These features were largely consistent between the two models.

An examination of moisture fluxes, their convergences, and precipitation over the Western Hemisphere

warm pool region in the NSIPP1 shows that the precipitation response (and thus latent heating) to an SST anomaly is preferentially located over the area of maximum climatological SST (i.e., the Western Hemisphere warm pool, Figs. 12 and 13). The location of the SLP maximum over the Gulf of Mexico is consistent with the Gill-type response to an off-equatorial heating anomaly (Gill 1980). Interestingly this response is not sensitive to the basin receiving the anomalous SST forcing, perhaps implicating the importance of the anomalous zonal and meridional SST gradients in generating this circulation feature (i.e., the structure of the SST forcing).

Inherent in any discussion of summertime precipitation variability over the continental United States is the inclusion of features related to the North American monsoon, particularly its influence on the upper-level circulation and the attendant negative phase relationship in precipitation between the southwestern United States and Great Plains. This phase relationship is recognized as the primary reason for the decay in Great Plains precipitation and LLJ during JAS in the mean seasonal cycle (Higgins et al. 1997a) and interannual variability (Higgins et al. 1998). However, the GPLLJ can form and exert its influence under many governing large-scale circulation regimes, including the presence of upper-level anticyclonic flow anomalies, as produced by the NAM. Notwithstanding the notable negative NAM–Great Plains phase relationship it is plausible that interactions of the NAM circulation features with the Great Plains may help to explain the higher correlation between the GPLLJ and precipitation during JAS. Higgins et al. (1997a) found that the NAM upper-level circulation features, which help to suppress precipitation over the Great Plains (i.e., the cause of the phase relationship), had no appreciable impact on the GPLLJ. So in effect it is conceivable that the GPLLJ becomes a dominant forcing mechanism for precipitation variability over the Great Plains during JAS as suggested in this study by the higher correlation between the GPLLJ and precipitation indices.

Of significant interest to the intra-American seas region is the presence of an SLP anomaly over the Gulf of Mexico, shown here linked to the GPLLJ in observations, AMIP simulations, and idealized Pacific and Atlantic SST forcing. Strengthening of SLP over the Gulf of Mexico has been noted before in the context of GPLLJ anomalies (Weaver and Nigam 2008). Given the regional focus of this SLP anomaly it appears not likely that a shift of the North Atlantic subtropical high (NASH) is the primary reason for the enhanced SLP, for a significant compensating effect (i.e., a comparable negative SLP anomaly) would appear over the central North Atlantic. While there exists a weak negative

correlation, the much stronger positive correlations over the subtropical Atlantic and especially the Gulf of Mexico allude to a mechanism producing a westward extension of the NASH, perhaps of local origin as suggested by the idealized SST experiments.

Given the limitations of relatively coarse-resolution global climate models in representing regional circulation features (i.e., the GPLLJ) and thermodynamic quantities relying on physical parameterizations (i.e., precipitation) (Ghan et al. 1996), it is necessary to be careful not to overindulge in attribution of physical mechanisms, especially in such a highly idealized setting with anomalous SST forcing at  $2\sigma$ . The purpose of imposing such highly anomalous forcing is to extract subtle linkages between SST and the mechanisms producing drought and pluvial over North America. Nevertheless, it is impossible to escape the link between global SST variability and regional low-level circulation features and precipitation demonstrated herein through the combined analysis of observations and model simulations.

*Acknowledgments.* This project was carried out as part of a U.S. CLIVAR Drought Working Group activity supported by NASA, NOAA, and NSF to coordinate and compare climate model simulations forced with a common set of idealized SST patterns. The authors thank NASA's Global Modeling and Assimilation Office (GMAO) for making the NSIPP1 runs available, the Lamont-Doherty Earth Observatory of Columbia University for making their CCM3 runs available, NOAA's Climate Prediction Center (CPC)/Climate Test Bed (CTB) for making the GFS runs available, NOAA's Geophysical Fluid Dynamics Laboratory (GFDL) for making the AM2.1 runs available, the National Center for Atmospheric Research (NCAR) for making the CAM3.5 runs available, and the Center for Ocean–Land–Atmosphere (COLA) and the University of Miami's Rosenstiel School of Marine and Atmospheric Science for making the CCSM3.0 coupled model runs available. The NASA/GMAO contributions to this project were supported by funding from the NASA Energy and Water Cycle Study (NEWS) program and the NASA Modeling and Analysis Program (MAP). The authors also thank three anonymous reviewers for their constructive comments, which greatly enhanced the quality of the manuscript.

#### REFERENCES

- Bacmeister, J. T., P. J. Pegion, S. D. Schubert, and M. J. Suarez, 2000: An atlas of seasonal means simulated by the NSIPP 1 atmospheric GCM. NASA Tech. Memo. 104606, Vol. 17, 191 pp.

- Barlow, M., E. H. Berbery, and S. Nigam, 1998: Evolution of the North American monsoon system. *J. Climate*, **11**, 1929–1947.
- , S. Nigam, and E. H. Berbery, 2001: ENSO, Pacific decadal variability, and U.S. summertime precipitation, drought, and stream flow. *J. Climate*, **14**, 2105–2128.
- Bates, G. T., M. P. Hoerling, and A. Kumar, 2001: Central U.S. springtime precipitation extremes: Teleconnections and relationships with sea surface temperature. *J. Climate*, **14**, 3751–3766.
- Bell, G. D., and J. E. Janowiak, 1995: Atmospheric circulation associated with the Midwest floods of 1993. *Bull. Amer. Meteor. Soc.*, **76**, 681–695.
- Berbery, E. H., and M. S. Fox-Rabinovitz, 2003: Multiscale diagnosis of the North American monsoon system using a variable-resolution GCM. *J. Climate*, **16**, 2238–2257.
- Bosilovich, M. G., and W. Y. Sun, 1999: Numerical simulation of the 1993 Midwestern flood: Land-atmosphere interactions. *J. Climate*, **12**, 1490–1505.
- Byerle, L. A., and J. Paegle, 2003: Modulation of the Great Plains low-level jet and moisture transports by orography and large-scale circulations. *J. Geophys. Res.*, **108**, 8611, doi:10.1029/2002JD003005.
- Ding, Q., and B. Wang, 2005: Circumglobal teleconnection in the Northern Hemisphere summer. *J. Climate*, **18**, 3483–3505.
- Ghan, S. J., X. Bian, and L. Corsetti, 1996: Simulation of the Great Plains low-level jet and associated clouds by general circulation models. *Mon. Wea. Rev.*, **124**, 1388–1408.
- Gill, A. E., 1980: Some simple solutions for heat-induced tropical circulation. *Quart. J. Roy. Meteor. Soc.*, **106**, 447–462.
- Helfand, M. H., and S. D. Schubert, 1995: Climatology of the simulated Great Plains low-level jet and its contribution to the continental moisture budget of the United States. *J. Climate*, **8**, 784–806.
- Higgins, R. W., Y. Yao, and X. L. Wang, 1997a: Influence of the North American monsoon system on the U.S. summer precipitation regime. *J. Climate*, **10**, 2600–2622.
- , —, E. S. Yarosh, J. E. Janowiak, and K. C. Mo, 1997b: Influence of the Great Plains low-level jet on summertime precipitation and moisture transport over the central United States. *J. Climate*, **10**, 481–507.
- , K. C. Mo, and Y. Yao, 1998: Interannual variability of the U.S. summer precipitation regime with emphasis on the southwestern monsoon. *J. Climate*, **11**, 2582–2606.
- , Y. Chen, and A. V. Douglas, 1999: Interannual variability of the North American warm season precipitation regime. *J. Climate*, **12**, 653–680.
- Holton, J. R., 1967: The diurnal boundary layer wind oscillation above sloping terrain. *Tellus*, **19**, 199–205.
- Kalnay, E., and Coauthors, 1996: The NCEP/NCAR 40-Year Reanalysis Project. *Bull. Amer. Meteor. Soc.*, **77**, 437–471.
- Kim, J., 2002: Precipitation variability associated with the North American monsoon in the 20th century. *Geophys. Res. Lett.*, **29**, 1650, doi:10.1029/2001GL014316.
- Mesinger, F., and Coauthors, 2006: North American Regional Reanalysis. *Bull. Amer. Meteor. Soc.*, **87**, 343–360.
- Rayner, N. A., D. E. Parker, E. B. Horton, C. K. Folland, L. V. Alexander, D. P. Rowell, E. C. Kent, and A. Kaplan, 2003: Global analyses of sea surface temperature, sea ice, and night marine air temperature since the late nineteenth century. *J. Geophys. Res.*, **108**, 4407, doi:10.1029/2002JD002670.
- Ruiz-Barradas, A., and S. Nigam, 2005: Warm season rainfall variability over the U.S. Great Plains in observations, NCEP and ERA-40 reanalyses, and NCAR and NASA atmospheric model simulations. *J. Climate*, **18**, 1808–1830.
- Saha, S., and Coauthors, 2006: The NCEP Climate Forecast System. *J. Climate*, **19**, 3483–3517.
- Schubert, S., M. H. Helfand, C.-Y. Wu, and W. Min, 1998: Subseasonal variations in warm-season moisture transport and precipitation over the central and eastern United States. *J. Climate*, **11**, 2530–2555.
- , M. J. Suarez, P. J. Pegion, M. A. Kistler, and A. Kumar, 2002: Predictability of zonal means during boreal summer. *J. Climate*, **15**, 420–434.
- , —, —, R. D. Koster, and J. T. Bacmeister, 2004: Causes of long term drought in the U.S. Great Plains. *J. Climate*, **17**, 485–503.
- , —, —, —, and —, 2008: Potential predictability of long-term drought and pluvial conditions in the U.S. Great Plains. *J. Climate*, **21**, 2919–2937.
- , and Coauthors, 2009: A U.S. CLIVAR project to assess and compare the responses of global climate models to drought-related SST forcing patterns: Overview and results. *J. Climate*, in press.
- Seager, R., Y. Kushnir, C. Herweijer, N. Naik, and J. Velez, 2005: Modeling of tropical forcing of persistent droughts and pluvials over western North America: 1856–2000. *J. Climate*, **18**, 4068–4091.
- Ting, M., and H. Wang, 1997: Summertime U.S. precipitation variability and its relation to Pacific sea surface temperature. *J. Climate*, **10**, 1853–1873.
- , and —, 2006: The role of the North American topography on the maintenance of the Great Plains summer low-level jet. *J. Atmos. Sci.*, **63**, 1056–1068.
- Wang, C., S.-K. Lee, and D. B. Enfield, 2007: Impact of the Atlantic warm pool on the summer climate of the Western Hemisphere. *J. Climate*, **20**, 5021–5040.
- Weaver, S. J., and S. Nigam, 2008: Variability of the Great Plains low-level jet: Large-scale circulation context and hydroclimate impacts. *J. Climate*, **21**, 1532–1551.
- , A. Ruiz-Barradas, and S. Nigam, 2009: Pentad evolution of the 1988 drought and 1993 flood over the Great Plains: An NARR perspective on the atmospheric and terrestrial water balance. *J. Climate*, in press.
- Wexler, H., 1961: A boundary layer interpretation of the low level jet. *Tellus*, **13**, 368–378.